

# Computational Stability Analysis of an Uncertain Bioreactor Model

Péter Polcz<sup>1</sup>, Gábor Szederkényi<sup>1,2</sup>, Katalin M. Hangos<sup>2</sup>

**Abstract** The computational stability analysis of a frequently used fermentation process model is reported in this paper. Linear fractional transformation (LFT) and computer algebra tools are used to transform the model into appropriate form. The Lyapunov function is searched in a general quadratic form composed of rational terms. The positivity of the Lyapunov function and the negativity of its derivative, respectively, are ensured through the solution of linear matrix inequalities (LMIs). The stability region is estimated by determining the level set of the Lyapunov function within a suitable convex domain. The stability analysis is performed for the controlled uncertain system with a linear proportional and integral substrate feedback considering different feedback gains. Computation results show that the studied simple linear feedback can guarantee stability in a wide neighborhood of the operating point.

## 1 Introduction

Approximating the domain of attraction is often a fundamental task in the analysis and control of nonlinear systems. The stability properties of dynamical systems are most often studied using Lyapunov functions. Therefore, an extensive literature exists on the computational construction of Lyapunov functions [2]. A fundamental result in this field is the existence of so-called maximal Lyapunov functions for a wide class of nonlinear systems and the

---

1. Faculty of Information Technology and Bionics, Pázmány Péter Catholic University, Práter u. 50/a, H1083 Budapest, Hungary

2. Institute for Computer Science and Control (MTA SZTAKI), Kende u. 13-17, H1111 Budapest, Hungary

*This work was supported by the National Research, Development and Innovation Office - NKFIH through grants No. 115694 and NF104706.*

corresponding (computationally demanding) iterative procedure to approximate them [16]. An algorithm for generating Lyapunov functions for a special class of nonlinear systems based on the construction of polytopes is given in [12]. In [6], a linear programming based method is given for the construction of Lyapunov functions for general planar nonlinear systems. During the last two decades, the use of linear matrix inequalities (LMI) and semidefinite programming (SDP) techniques for the stability analysis of nonlinear systems has become popular due to their advantageous properties and the availability of efficient numerical solvers. A recent important result from this line of research is published in [1], where the authors use Finsler's lemma and affine parameter dependent LMIs to compute rational Lyapunov functions for a wide class of locally asymptotically stable nonlinear systems.

Recently introduced sufficient conditions for the stability are affine parameter dependent LMIs, since they are characterized by affine functions of the state ( $x$ ) and uncertain parameters ( $\delta$ ). Affine parameter dependent LMIs can be computationally handled by checking their feasibility at the corner points (vertices) of a polytopic region, on which the uncertain parameters are defined. In [1] it is shown that with some additional conservatism, the use of the vertices could be avoided by modifying the LMIs with the S-Procedure.

It is known that bioreactors often show strongly nonlinear dynamical behaviour and their efficient control is a challenging task [5]. Still, there exist successful approaches for ensuring optimal biomass production even when the growth kinetics is uncertain [7]. It is, however, widely believed that linear control structure can hardly guarantee acceptable performance and wide-enough stability region for the closed loop system. In [4], a Lyapunov-function-based stability analysis of a simple continuous fermentation process is performed assuming static linear state feedbacks. The stability region of similar bioreactor models was analyzed in [15] using maximal Lyapunov functions.

In this work, we use a slightly modified version of the method [1] for the stability analysis of a frequently used bioreactor model [4] assuming a simple linear control structure and uncertainty of the maximal growth rate in the kinetics. The main motivation of our work was to evaluate the applicability of the approach [1] on an uncertain kinetic model, and to study the effect of a linear substrate feedback knowing that most of the advanced nonlinear control methods require full state information, while the satisfactory measurement of biomass concentration is often difficult in practice [9].

## 2 Background

In this section, we present the basic notions and results on which our computational method is based.

**System class, Lyapunov functions, and the domain of attraction.**

We consider nonlinear systems of the form

$$\dot{x}(t) = f(x(t), \delta(t)) \quad x(t) \in \mathcal{X}, \quad x_0 \in \mathcal{X}, \quad \delta(t) \in \mathcal{D}, \quad \dot{\delta}(t) \in \check{\mathcal{D}} \quad (1)$$

where  $\mathcal{X} \subset \mathbb{R}^n$  and  $\mathcal{D}, \check{\mathcal{D}} \subset \mathbb{R}^d$  are given polytopes,  $x$  is the state vector function,  $x_0 = x(0)$  is the initial condition, and  $\delta$  is a smooth, bounded vector function with bounded time derivative representing the uncertain parameters. Henceforth, the time arguments of  $x$  and  $\delta$  will be suppressed as it is commonly done in the literature. Furthermore,  $f: \mathbb{R}^n \times \mathcal{D} \mapsto \mathbb{R}^n$  of Eq. (1) is a well defined smooth *rational mapping*, with the property  $f(0, \delta) = 0$  for all  $\delta \in \mathcal{D}$ , i.e.,  $x^* = 0 \in \mathbb{R}^n$  is a locally asymptotically stable equilibrium point of (1) for all  $\delta \in \mathcal{D}$ . The set of all initial conditions, from which the solutions converge to  $x^*$  is called the *domain of attraction* (DOA).

We are looking for an appropriate rational Lyapunov function  $V(x, \delta)$  which satisfies the following conditions:

$$\begin{aligned} v_l(x) \leq V(x, \delta) \leq v_u(x) & \quad \forall (x, \delta) \in \mathcal{X} \times \mathcal{D} \\ \dot{V}(x, \delta, \dot{\delta}) \leq -v_d(x) & \quad \forall (x, \delta, \dot{\delta}) \in \mathcal{X} \times \mathcal{D} \times \check{\mathcal{D}} \end{aligned} \quad (2)$$

where  $v_l$ ,  $v_u$  and  $v_d$  are continuous positive functions on  $\mathcal{X}$ . Clearly, if the inequalities in (2) are fulfilled, then any closed level set of  $V$  contained (entirely) in  $\mathcal{X}$  bounds an invariant region of the state space that is part of the DOA. Roughly speaking, our main objective is to find a function  $V(x, \delta)$  having a level set, which bounds the largest possible invariant region.

**Dynamical system representation.** In [1], the authors are looking for a Lyapunov function in the form

$$V(x, \delta) = \pi_b^T(x, \delta) P \pi_b(x, \delta), \quad \pi_b = \begin{bmatrix} x \\ \pi \end{bmatrix} \quad (3)$$

where  $P \in \mathbb{R}^{m \times m}$  is a *constant symmetric* matrix, not necessarily positive definite, and  $\pi: \mathbb{R}^n \times \mathcal{D} \mapsto \mathbb{R}^p$  is a mapping, in which each element is a monomial in  $(x, \delta)$ , or a smooth rational function with monomial numerator. The arguments of  $\pi$  and  $\pi_b$  will be suppressed below.

Using the variables from Eqs. (1) and (3), we present a similar differential-algebraic representation of nonlinear models that was introduced in [1]:

$$\begin{aligned} \dot{x} = f(x, \delta) = Ax + B\pi & \quad x_0 \in \mathcal{X} \\ 0 = \mathcal{N}_{\pi_b}(x, \delta)\pi_b & \quad \delta \in \mathcal{D}, \quad \dot{\delta} \in \check{\mathcal{D}} \end{aligned} \quad (4)$$

where  $A \in \mathbb{R}^{n \times n}$  and  $B \in \mathbb{R}^{n \times p}$  are constant matrices.

The representation (4) separates the linear part of the system ( $x$ ) from its nonlinear part ( $\pi$ ). The application of the linear fractional transformation (LFT) and further algebraic steps are proposed in [13] to transform the sys-

tem  $\dot{x} = \mathcal{A}(x, \delta)x$  into the desired representation  $\dot{x} = Ax + B\pi$  in Eq. (4), and to generate an appropriate annihilator  $\mathcal{N}_{\pi_b}(x, \delta)$ . These transformations also result in the dimension reduction of the optimization problem compared to the results presented in [1].

### 3 The SDP problem for estimating the domain of attraction

In this section, we present the key elements of the method to construct the semidefinite optimization task for obtaining an appropriate rational Lyapunov function and its maximal invariant level set  $\varepsilon_\alpha$  as an estimate of the true domain of attraction.

Using this model representation, we are searching for a Lyapunov function of the form (3), which satisfies the conditions (2) for every  $(x, \delta, \dot{\delta}) \in \mathcal{X} \times \mathcal{D} \times \check{\mathcal{D}}$ . As Fig. 1 illustrates, we define an auxiliary polytope  $\mathcal{Y}$  around the locally stable origin inside  $\mathcal{X}$ , looking for a level set  $\varepsilon_\alpha = \{x \in \mathcal{X} \mid V(x) = \alpha, 1 \leq \alpha\}$  that is inside  $\mathcal{X}$ , while  $\varepsilon_1$  is outside of  $\mathcal{Y}$ . In order to find the maximal invariant level set  $\varepsilon_\alpha$  of the Lyapunov function, one should maximize  $\alpha$ , under the following conditions

- (C1)  $V(x, \delta)$  is positive on  $\mathcal{X} \times \mathcal{D}$
- (C2)  $\dot{V}(x, \delta, \dot{\delta})$  is negative on  $\mathcal{X} \times \mathcal{D} \times \check{\mathcal{D}}$
- (C3)  $\varepsilon_\alpha$  lies inside  $\mathcal{X}$
- (C4)  $\mathcal{Y}$  is inside  $\varepsilon_1$  (without this condition the function  $V(x)$  can be scaled arbitrarily leading to an unbounded feasible solution).

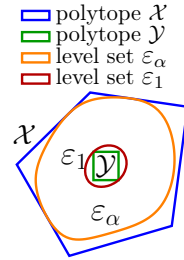


Fig. 1

In the following subsections, we formulate LMI conditions for each constraint.

**Positivity of the Lyapunov function.** Using an annihilator and applying Finsler's lemma [13, Lemma 2.1], one can formulate a sufficient *affine parameter dependent* LMI condition for the positivity of the Lyapunov function (3) (which is less conservative than simply prescribing  $P > 0$ ) as follows:

$$\exists L_b \in \mathbb{R}^{m \times q} : P + L_b \mathcal{N}_{\pi_b}(x, \delta) + \mathcal{N}_{\pi_b}^T(x, \delta) L_b^T > 0, \forall (x, \delta) \in \vartheta(\mathcal{X} \times \mathcal{D}), \quad (5)$$

where the decision variables are matrices  $P$  and  $L_b$ , furthermore,  $\vartheta$  denotes the corner points of a convex polytope (see [3, Prop. 5.4]).

In [1], two different annihilators of  $\pi_b$  are used, namely  $C_b(x, \delta)$  and  $\mathcal{N}_{\pi_b}(x, \delta)$ , having two different roles. For the sake of simplicity, we propose to unite these two annihilators into a single one:  $\mathcal{N}_{\pi_b}(x, \delta) = \begin{bmatrix} C_b(x, \delta) \\ \mathcal{N}_{\pi_b}(x, \delta) \end{bmatrix}$ , as it is visible in Eq. (5).

**Negativity of the time derivative of the Lyapunov function.** The time derivative of  $V(x, \delta)$  is expressed as  $\dot{V}(x, \delta, \dot{\delta}) = \pi_a^T (P_a + P_a^T) \pi_a$ , where  $\pi_a : \mathcal{X} \times \mathcal{D} \times \check{\mathcal{D}} \mapsto \mathbb{R}^{n+2p+n^2+np}$  is a smooth rational mapping (the arguments of  $\pi_a$  are suppressed),  $P_a$  is a square matrix with appropriate dimensions. The variables  $\pi_a$  and  $P_a$  are defined in [1] in Eqs. (57) and (39), respectively.

Using the model matrices  $A, B, \mathcal{N}_{\pi_b}(x, \delta)$  from representation (4), we can construct an annihilator  $\mathcal{N}_{\pi_a}(x, \delta, \dot{\delta})$ , such that  $\mathcal{N}_{\pi_a}(x, \delta, \dot{\delta}) \pi_a = 0$  for all  $(x, \delta, \dot{\delta}) \in \mathbb{R}^{n+2d}$ . The exact construction of  $\mathcal{N}_{\pi_a}(x, \delta, \dot{\delta})$  is presented in technical report [14, Eq. (3.22)]. The negative definiteness of  $\dot{V}(x, \delta, \dot{\delta})$  is ensured by the following sufficient *affine parameter dependent* LMI condition:

$$\begin{aligned} \exists L_a \in \mathbb{R}^{(n+2p+n^2+np) \times (2q+n^2+nq)}, \quad \text{such that:} \quad (6) \\ P_a + P_a^T + L_a \mathcal{N}_{\pi_a}(x, \delta, \dot{\delta}) + \mathcal{N}_{\pi_a}^T(x, \delta, \dot{\delta}) L_a^T < 0, \quad \forall (x, \delta, \dot{\delta}) \in \vartheta(\mathcal{X} \times \mathcal{D} \times \check{\mathcal{D}}) \end{aligned}$$

where  $P_a$  and  $L_a$  contain the decision variables and  $P$  can be directly obtained from  $P_a$  [1].

**SDP conditions on  $\mathcal{X}$  and  $\mathcal{Y}$ .** As it was mentioned, we require the level set  $\varepsilon_\alpha$  to be located inside  $\mathcal{X}$ , this constraint is equivalent to the inequality  $V(x, \delta) > \alpha$  for every  $\delta \in \mathcal{D}$  and for every  $x$  on the boundary of  $\mathcal{X}$ . According to Finsler's lemma, a sufficient LMI condition can be expressed for this inequality as

$$\begin{aligned} \forall k = \overline{1, M_{\mathcal{X}}}: \exists L_{c_k} \in \mathbb{R}^{m \times q}, \quad \exists M_{c_k} \in \mathbb{R}^{(m+1) \times n}, \quad \text{such that:} \quad (7) \\ Q_k^T P_{c_k}^{(\alpha)}(x, \delta) Q_k \geq 0, \quad \forall (x, \delta) \in \vartheta(\mathcal{F}_k^{(\mathcal{X})} \times \mathcal{D}), \end{aligned}$$

where  $M_{\mathcal{X}}$  is the number of facets of  $\mathcal{X}$ ,  $\mathcal{F}_k^{(\mathcal{X})}$  denotes the  $k$ th facet of  $\mathcal{X}$  and the constant matrix  $Q_k$  is given in [1, Eq. (87)]. The *affine* matrix function  $P_{c_k}^{(\alpha)}$  is defined as follows:

$$P_{c_k}^{(\alpha)}(x, \delta) = \begin{bmatrix} P + L_{c_k} \mathcal{N}_{\pi_b}(x, \delta) + \mathcal{N}_{\pi_b}^T(x, \delta) L_{c_k}^T & 0 \\ 0 & -\alpha \end{bmatrix} + M_{c_k} \mathcal{N}_{\pi_c}(x) + \mathcal{N}_{\pi_c}^T(x) M_{c_k}^T$$

where  $\mathcal{N}_{\pi_c}(x) = [I_n \ 0_{n \times m} \ -x]$ . Matrix  $P$ ,  $L_{c_k}$ ,  $M_{c_k}$  and the scalar  $\alpha$  are the decision variables. Similarly, the last condition ( $\mathcal{Y}$  lies inside  $\varepsilon_1$ ) can be formulated as:

$$\begin{aligned} \forall k = \overline{1, M_{\mathcal{Y}}}: \exists \bar{L}_{c_k} \in \mathbb{R}^{m \times q}, \quad \exists \bar{M}_{c_k} \in \mathbb{R}^{(m+1) \times n}, \quad \text{such that:} \quad (8) \\ \bar{Q}_k^T \bar{P}_{c_k}^{(1)}(x, \delta) \bar{Q}_k \leq 0, \quad \forall (x, \delta) \in \vartheta(\mathcal{F}_k^{(\mathcal{Y})} \times \mathcal{D}) \end{aligned}$$

Finally, we have to maximize  $\alpha$  subject to the inequality constraints (5), (6), (7), (8), in order to find an appropriate Lyapunov function and its maximal invariant level set. This method is presented in detail in [14, Chapter 3].

**Estimating the ‘robust DOA’.** Generally, the uncertain parameters  $\delta$  appear in the computed Lyapunov function, hence the need arises to estimate the so-called *robust DOA*, that is the set of initial conditions, from which the system converges to the equilibrium point for all possible values of the uncertain parameters. The robust invariant region (denoted by  $\varepsilon_\alpha^*$ ) is computed as the intersection of the bounded regions of the maximal invariant level sets for all possible values of  $\delta$ , namely,  $\varepsilon_\alpha^* = \bigcap_{\delta \in \mathcal{D}} \{x \in \mathcal{X} \mid V(x, \delta) \leq \alpha\}$ .

**Finding an appropriate outer polytope.** We applied an iterative procedure in order to algorithmically find a suitable polytope  $\mathcal{X}$ , on which the Lyapunov conditions are tested. First of all, an invariant level set  $\varepsilon_\alpha^{(0)}$  is found by solving the optimization task considering a relatively small initial polytope  $\mathcal{X}^{(0)}$ . Then, in each  $i$ th iteration step a new polytope  $\mathcal{X}^{(i+1)}$  is defined considering the shape of the level set  $\varepsilon_\alpha^{(i)}$ .

In this work, we require  $\mathcal{X}$  to be a rectangular polytope  $\mathcal{X} = [x_{11}, x_{12}] \times [x_{21}, x_{22}] \times \dots \times [x_{n1}, x_{n2}]$  (not necessarily symmetric with respect to the origin), which is enlarged by iterations using some scaling coefficients  $\kappa_i$ . This assumption can be advantageous in case of higher dimensional systems, because generating a new polytope  $\mathcal{X}^{(i+1)}$  is quite straightforward by considering the axis aligned bounding box of  $\varepsilon_\alpha^{(i)}$ . We additionally mention the fact that, in this way, we can avoid handling arbitrarily shaped closed (hyper) triangle meshes.

In order to simplify the equations, we introduce the following notation. We collect the coordinates of the corner points of  $\mathcal{X}$  in a matrix  $X = \begin{bmatrix} x_{11} & x_{12} & \dots & x_{n1} \\ x_{21} & x_{22} & \dots & x_{n1} \end{bmatrix}$ . The scale coefficients  $\kappa_i \in (1, 2)$ ,  $i = \overline{1, 2n}$  are gathered in a vector  $\kappa \in (1, 2)^{2n}$ . The algorithm of the polytope evaluation is the following:

```

X = initial polytope X(0)
for i = 1 to maximum nr of iterations do
  Solve the SDP problem for X  $\implies$  maximal invariant level set  $\varepsilon_\alpha$ 
  if solution found then
    X(prev) = bounding box of  $\varepsilon_\alpha$ 
    increase the values of  $\kappa_i$ :  $\kappa_i = \frac{\kappa_i + 2}{2}$ ,  $i = \overline{1, 2n}$ 
  else
    decrease the values of  $\kappa_i$ :  $\kappa_i = \frac{\kappa_i + 1}{2}$ ,  $i = \overline{1, 2n}$ 
  end
  Increase-polytope- $\mathcal{X}(X^{(prev)}, \kappa)$ 
end
Function Increase-polytope- $\mathcal{X}(X, \kappa)$ 
  |  $X_{i1} = \max(X_{i1}\kappa_{2i-1}, x_i^{(min)})$  ,  $X_{i2} = X_{i2}\kappa_{2i}$ ,  $i = \overline{1, n}$ 
end

```

**Algorithm 1:** Evaluate the polytope  $\mathcal{X}$

The constant variables  $x_i^{(min)}$  have a significance only when considering non-

negative systems, furthermore, we assume that using the initial polytope  $\mathcal{X}^{(0)}$  results in a feasible SDP problem.

## 4 Model of the continuous fermentation process

In this section, we present an isothermal nonlinear continuous fermentation process model taken from [4] with constant volume  $V$ , constant physico-chemical properties and uncertain maximal growth rate  $\delta = \mu_{max}$ . The reaction rate of the fermentation  $\mu(S)$  is a rational function, where  $\mu_{max}$  can be considered as its principal reaction rate coefficient. This value is usually determined experimentally with relatively high uncertainty, causing a multiplicative uncertainty factor in Eq. (9).

In the numerical calculations, we assumed that  $\delta$  belongs to the interval  $\mathcal{D} = [0.8, 1.2]$ , and let the nominal value of  $\delta$  be:  $\delta_0 = 1$  [l/h].

The dynamics of the process is given by the state-space model

$$\begin{aligned} \frac{dX}{dt} &= \mu(S)X - \frac{XF}{V}, & \frac{dS}{dt} &= -\frac{\mu(S)X}{Y} + \frac{(S_F - S)F}{V}, & V &= 4 \text{ [l]}, & Y &= 0.5 \\ \mu(S) &= \mu_{max} \frac{S}{K_2 S^2 + S + K_1} & & & S_F &= 10 \text{ [g/l]} \\ & & & & K_1 &= 0.03 \text{ [g/l]} \\ & & & & K_2 &= 0.5 \text{ [l/g]} \end{aligned} \quad (9)$$

where the state variables  $X$  and  $S$  are the biomass and substrate concentrations, respectively,  $F$  is the feed flow rate,  $S_F$  is the substrate feed concentration,  $Y$  is the yield coefficient,  $K_1$  and  $K_2$  are the saturation and inhibition parameters, respectively. For more details on the bioreactor model, see [4].

The above model can easily be written in standard input-affine form with the centered state vector

$$x = [x_1 \ x_2]^T = [X - X_0 \ S - S_0]^T \quad (10)$$

consisting of the centered biomass and substrate concentrations. The centered input flow rate is chosen as manipulate input variable  $u = F - F_0(\delta)$ , where the inlet feed flow rate  $F_0$  is a linear function of  $\delta$ . The centered model is:  $\dot{x} = f(x, \delta) + g(x)u$ , where

$$f(x, \delta) = \begin{bmatrix} (x_1 + X_0) \cdot \mu(x_2 + S_0) & -\frac{(x_1 + X_0)F_0(\delta)}{V} \\ -\frac{(x_1 + X_0) \cdot \mu(x_2 + S_0)}{Y} & + \frac{(S_F - (x_2 + S_0))F_0(\delta)}{V} \end{bmatrix} \quad (11)$$

$$g(x) = -\frac{1}{V} \begin{bmatrix} x_1 + X_0 \\ x_2 + S_0 - S_F \end{bmatrix} \quad (12)$$

Function  $f$  can also be written in the form  $f(x, \delta) = \mathcal{A}_1(x, \delta)x$ , where

$$\mathcal{A}_1(x, \delta) = \begin{bmatrix} -\frac{F_0(\delta)(c_2x_2^2+c_1x_2)}{q(x_2)V} & \frac{\delta V(x_1+X_0)-X_0F_0(\delta)(c_2x_2+c_1)}{q(x_2)V} \\ -\frac{\delta S_0}{q(x_2)Y} & -\frac{F_0(\delta)}{V} - \frac{\delta(x_1+X_0)}{q(x_2)Y} - \frac{F_0(\delta)(S_0-S_F)(c_2x_2+c_1)}{q(x_2)V} \end{bmatrix}$$

$$c_0 = K_2S_0^2 + S_0 + K_1 \quad c_1 = 2K_2S_0 + 1 \quad (13)$$

$$q(x_2) = c_2x_2^2 + c_1x_2 + c_0 \quad c_2 = K_2$$

The equilibrium point of the system is computed such that the biomass production  $X_0F_0$  is maximized:

$$S_0 = \arg \max_{S>0} (S_F - S)\mu(S) = \frac{-K_1 + \sqrt{K_1^2 + S_F^2 K_1 K_2 + S_F K_1}}{K_2 S_F + 1} \quad (14)$$

$$X_0 = (S_F - S_0)Y, \quad F_0(\delta) = V\mu(S_0) \quad (15)$$

The identities in Eq. (15) are coming from the fact that  $f(0, \delta) = 0$  for all  $\delta$ . We can observe, that the equilibrium point of the system does not dependent on  $\delta$ . The steady state operating point values are  $X_0 = 4.8907 [g/l]$ ,  $S_0 = 0.2187 [g/l]$  and  $F_0(\delta) = 3.2089 \cdot \delta [l/h]$ . Due to the positivity of the biomass and substrate concentrates, we can assume that  $x_1 > -X_0$  and  $x_2 > -S_0$ .

## 5 Stability analysis results

In this section, we present the computational results of the method described in the first part of this paper.

The results presented in this section have been computed in the Matlab environment. For symbolic computations we used the Matlab's built-in Symbolic Math Toolbox based on Mupad. For LFT we used the Enhanced LFR-toolbox [8, 11]. To model and solve semidefinite optimization (SDP) problems we used the Mosek solver with YALMIP [10].

### 5.1 Linear proportional substrate feedback

Let us define the centered input flow rate as  $u = -k_P x_2$ , where  $k_P > 0$  is the feedback gain. The equation of the closed-loop system can be transformed into the following form:  $\dot{x} = \mathcal{A}_2(x, \delta)x$ , where

$$\mathcal{A}_2(x, \delta) = (\mathcal{A}_1(x, \delta) - g(x)K_P)x, \quad K_P = [0 \ k_P] \quad (16)$$

Having this form, we can apply the LFT to the matrix function  $\mathcal{A}_2(x, \delta)$ , then executing the consecutive algebraic transformations presented in [13], we can obtain the necessary representation (4). When estimating the DOA,



we tested different feedback gain values from the interval  $k_P \in [0.125, 5.125]$ . In Fig. 5, we can see the estimated DOA for each tested value of  $k_P$ . We can observe, that between the values  $k_P^{(1)} = 0.916$  ( $A^{(1)} = 0.6634$ ) and  $k_P^{(2)} = 0.917$  ( $A^{(2)} = 6.5188$ ) the estimated DOA suddenly increases.

In Fig. 2, we can see the obtained maximal robust invariant region and the corresponding rectangular polytope  $\mathcal{X}$  for different feedback gain values. The polytope  $\mathcal{X}$  is evaluated automatically as presented in Algorithm 1, where the numerical values of the scaling coefficients are:  $\kappa_1 = \kappa_2 = 1.5$ ,  $\kappa_3 = 1.4$ ,  $\kappa_4 = 1.6$ . Fig. 3. illustrates the estimate for a manually chosen polytope, when  $k_P = 0.917$ . For that polytope we achieved an even larger invariant region than that when using a rectangular polytope and applying the same feedback gain value.

The largest area is obtained when  $k_P = 0.917$ . The approximated values of the obtained model matrices in this case are the following:

$$\begin{aligned} \pi^T &= \left[ \frac{\delta x_1}{\zeta(x_2)} \quad \frac{\delta x_2}{\zeta(x_2)} \quad \delta x_2 \quad \frac{\delta x_1 x_2}{\zeta(x_2)} \quad x_1 x_2 \quad \frac{\delta x_1 x_2^2}{\zeta(x_2)} \quad \frac{x_1 x_2^2}{\zeta(x_2)} \quad \frac{x_1 x_2}{\zeta(x_2)} \quad \frac{x_2^3}{\zeta(x_2)} \quad \frac{x_2^2}{\zeta(x_2)} \quad \frac{\delta x_2^2}{\zeta(x_2)} \quad x_2^2 \right] \\ A &= \begin{bmatrix} 0 & 1.121 \\ 0 & -2.242 \end{bmatrix}, \quad \zeta(x_2) = \frac{q(x_2)}{c_2} = \frac{q(x_2)}{K_2} \\ B &= \begin{bmatrix} 0 & 0.219 & 0 & 4.47e-2 & 0.229 & -0.802 & 0 & 0 & 0 & -3.92 & 0 \\ -0.875 & -0.437 & -0.802 & -4 & 0 & 0 & 0 & 0 & 0 & 7.85 & 0.229 \end{bmatrix} \end{aligned} \quad (17)$$

The generated annihilator  $\mathcal{N}_{\pi_b}$  has  $q = 21$  rows, therefore, we do not present it here. Fig. 4 illustrates the obtained Lyapunov function  $V(x, \delta)$  in two different view points when  $\delta = \delta_0$ .

In [13], the estimated DOA is already shown in the case of an open-loop bioreactor system with no uncertainty. We can remark that assuming even a simple substrate feedback law with an appropriate feedback gain, the area of the estimate is much larger compared to that obtained for the open-loop system in [14].

## 5.2 Linear proportional and integral substrate feedback

Let the centered input flow rate be  $u = -k_P x_2 - k_I \int_{t_0}^t x_2(\tau) d\tau$ . In this case the equation of the closed-loop system is  $\dot{\xi} = \mathcal{A}_3(x, \delta)\xi$ , where  $\xi = [x_1 \ x_2 \ u]^T$  is the state vector of the obtained three dimensional system. Using the variables from Eqs. (12) and (13), the state-transition matrix function  $\mathcal{A}_3$  can be composed as follows:

$$\mathcal{A}_3(x, \delta) = \begin{bmatrix} \mathcal{A}_1(x, \delta) & g(x) \\ -K_P \mathcal{A}_1(x, \delta) - K_I & -K_P g(x) \end{bmatrix} \in \mathbb{R}^{3 \times 3}, \quad \begin{matrix} K_P = [0 \ k_P] \\ K_I = [0 \ k_I] \end{matrix} \quad (18)$$

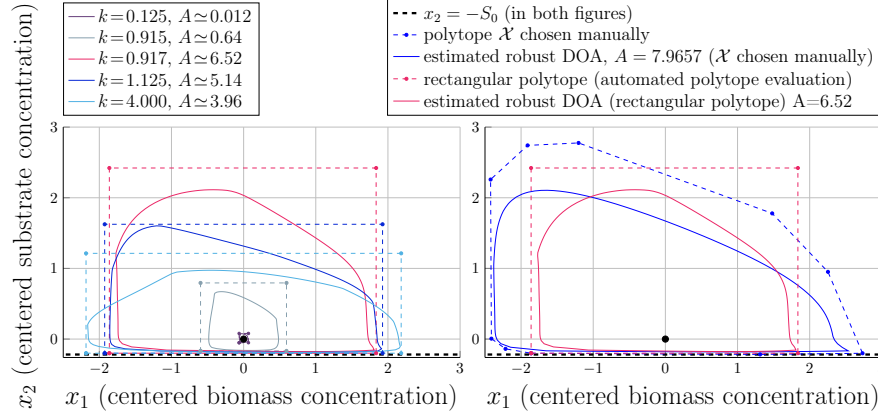


**Fig. 2** The estimated robust DOA (solid lines) and the corresponding rectangular polytope  $\mathcal{X}$  (dashed lines) for different feedback gain values, with an automatic polytope ( $\mathcal{X}$ ) selection.

**Fig. 3** The estimated robust DOA, when the polytope  $\mathcal{X}$  was chosen manually (blue line) and when a rectangular  $\mathcal{X}$  is evaluated automatically (red line). In both cases, the feedback gain is  $k = 0.917$ .

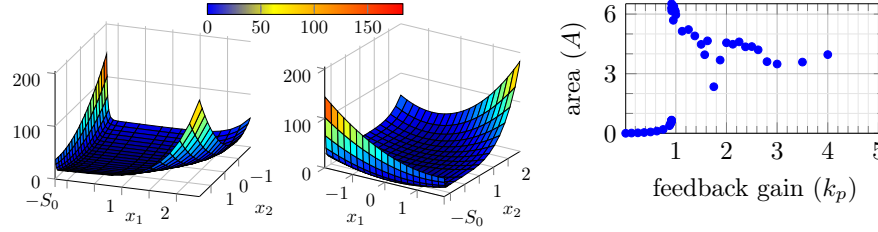


**Fig. 4** Plot of the Lyapunov function  $V(x, \delta)$  from two different angles, when  $k = 0.917$  and  $\delta = \delta_0$ .

**Fig. 5** The area of the computed robust DOA for different  $k_p$  feedback gain values.

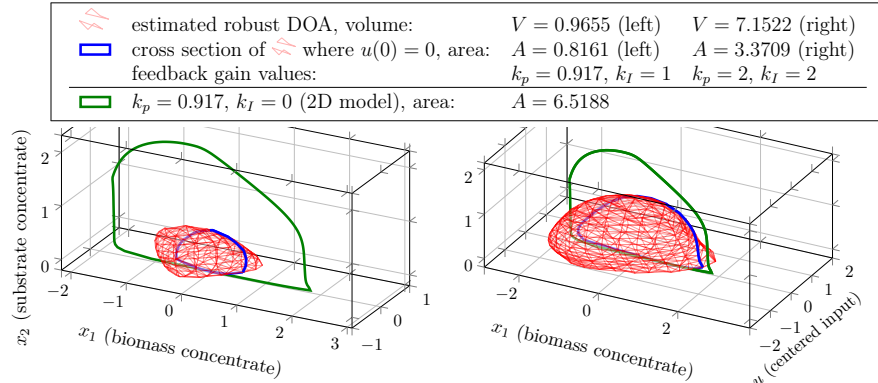


**Fig. 6** The computed robust DOA in case of two different feedback gain configurations, when an additional integral substrate feedback is applied. In both cases, the figure illustrates the used polytope  $\mathcal{X}$  (bounding box), the maximal robust invariant region (red mesh) and its cross section when  $u(0) = 0$  (blue line).

After the model transformation steps, the approximated value of the model matrices  $[A|B]$  and column vector  $\pi$  are the following:

$$\begin{bmatrix} 0 & 0 & -1.22 & | & 0 & 0.219 & 0 & 0.0447 & -0.25 & -0.802 & 0 & 0 & 0 & 0 & -3.92 & 0 \\ 0 & 0 & 2.45 & | & -0.875 & -0.437 & -0.802 & -4.0 & 0 & 0 & 0 & 0 & 0 & 0 & 7.85 & -0.25 \\ 0 & -2.0 & -4.89 & | & 1.75 & 0.875 & 1.6 & 8.0 & 0 & 0 & 0 & 0 & 0 & 0 & -15.7 & 0.5 \end{bmatrix}$$

$$\pi^T = \left[ \frac{\delta x_1}{\zeta(x_2)} \quad \frac{\delta x_2}{\zeta(x_2)} \quad \delta x_2 \quad \frac{\delta x_1 x_2}{\zeta(x_2)} \quad x_1 x_3 \quad \frac{\delta x_1 x_2^2}{\zeta(x_2)} \quad \frac{x_1 x_2^2}{\zeta(x_2)} \quad \frac{x_1 x_2}{\zeta(x_2)} \quad \frac{x_2^3}{\zeta(x_2)} \quad \frac{x_2^2}{\zeta(x_2)} \quad \frac{\delta x_2^2}{\zeta(x_2)} \quad x_2 x_3 \right]$$

The obtained annihilator has  $q = 22$  rows. Fig. 6. illustrates the obtained robust invariant 3D region in two different feedback gain configurations, and its cross section when the initial value of the input variable is zero. We can observe that the obtained estimates in both feedback configurations are much smaller than that obtained when no integral feedback is applied. A possible cause of this artifact could be that the dimensions of optimization problem corresponding to the three dimensional system are significantly larger, hence it becomes a more complex task for the optimization solver.

When evaluating the polytope  $\mathcal{X}$  we used Algorithm 1, but we have fixed the bounds of the centered input feed flow rate in both feedback configurations as  $u \in [-1, 1]$  (Fig. 6, left) and  $u \in [-2, 2]$  (Fig. 6, right), respectively.

## 6 Conclusions

In this work, we presented an improved optimization-based computational method for determining Lyapunov functions and invariant regions for nonlinear dynamical systems with rational terms based on [1]. We gave a simplified formula for the LMIs of the optimization problem by merging the two annihilators defined in [1] into a single one:  $\mathcal{N}_{\pi_b}(x, \delta)$ . Furthermore, we presented an algorithm to evaluate the initial polytope  $\mathcal{X}^{(0)}$ , on which the Lyapunov conditions are tested. We applied the method for the stability analysis of an uncertain continuous bioreactor model.

The Lyapunov function for the closed-loop system using a proportional state feedback law was successfully computed, and the corresponding guaranteed stability regions were determined for different feedback gains. The method was successfully applied on the three dimensional uncertain closed-loop system considering a proportional and an integral substrate feedback law. The computational approach itself is able to handle a wide class of uncertain models, therefore future work will be focused on the stability analysis of more complex and/or higher dimensional systems.

## References

1. A. Trofino and T. J. M. Dezuo. LMI stability conditions for uncertain rational nonlinear systems. *International Journal of Robust and Nonlinear Control*, 2013.
2. G. Chesi. *Domain of attraction: analysis and control via SOS programming*, volume 415. Springer Science & Business Media, 2011.
3. C. Scherer and S. Weiland. Linear matrix inequalities in control. *Lecture Notes, Dutch Institute for Systems and Control, Delft, The Netherlands*, 2000.
4. G. Szederkényi, N. R. Kristensen, K. M. Hangos, and S. B. Jorgensen. Nonlinear analysis and control of a continuous fermentation process. *Computers and Chemical Engineering*, 26:659–670, 2002.
5. D. Dochain, M. Perrier, and M. Guay. Extremum seeking control and its application to process and reaction systems: A survey. *Mathematics and Computers in Simulation*, 82:369–380, 2011.
6. P. Giesl and S. Hafstein. Construction of Lyapunov functions for nonlinear planar systems by linear programming. *Journal of Mathematical Analysis and Applications*, 388:463–479, 2012.
7. M. Guay, D. Dochain, and M. Perrier. Adaptive extremum seeking control of continuous stirred tank bioreactors with unknown growth kinetics. *Automatica*, 40:881–888, 2004.
8. S. Hecker, A. Varga, and J-F. Magni. Enhanced LFR-toolbox for MATLAB. pages 25–29, 2004.
9. A. Hocalar, M. Turker, C. Karakuzu, and U. Yuzgec. Comparison of different estimation techniques for biomass concentration in large scale yeast fermentation. *ISA Transactions*, 50:303–314, 2011.
10. J. Lofberg. Yalmip : A toolbox for modeling and optimization in MATLAB. In *Proceedings of the CACSD Conference*, Taipei, Taiwan, 2004.
11. J-F. Magni. Linear fractional representation toolbox (version 2.0) for use with matlab. *Free Web publication <http://www.cert.fr/dcsd/idco/perso/Magni>*, 2006.
12. Y. Ohta, H. Imanishi, L. Gong, and H. Haneda. Computer generated Lyapunov functions for a class of nonlinear systems. *IEEE Transactions on Circuits and Systems*, 40:343–354, 1993.
13. P. Polcz, G. Szederkényi, and T. Péni. An improved method for estimating the domain of attraction of nonlinear systems containing rational functions. In *Journal of Physics: Conference Series*, volume 659, page 012038. IOP Publishing, 2015.
14. P. Polcz and G. Szederkényi. An improved method for estimating the domain of attraction of uncertain rational systems using linear matrix inequality conditions and SDP optimization. Technical report, Faculty of Information Technology and Bionics, Pázmány Péter Catholic University, Práter u. 50/a, H1083 Budapest, Hungary, April 2016. Available at <http://users.itk.ppke.hu/~polpe/techreport2016apr.pdf>.
15. Sz. Rozgonyi, K. M. Hangos, and G. Szederkényi. Determining the domain of attraction of hybrid non-linear systems using maximal Lyapunov functions. *Kybernetika*, 46:19–37, 2010.
16. A. Vannelli and M. Vidyasagar. Maximal Lyapunov functions and domains of attraction for autonomous nonlinear systems. *Automatica*, 21:69–80, 1985.